Linear augmented-Slater-type-orbital method for electronic-structure calculations. III. Structural and cohesive energies of the 5*d* elements Lu—Au

J. W. Davenport, R. E. Watson, and M. Weinert
Department of Physics, Brookhaven National Laboratory, Upton, New York 11973
(Received 22 March 1985)

The linear augmented-Slater-type-orbital method is applied to the electronic band structures of the 5*d* transition metals Lu through Au. Scalar relativistic, muffin-tin potential, and local density calculations are performed for each metal in both the fcc and bcc structures. Special sets of **k** points are used and the variation in crystal total energy as a function of mesh density ($\approx$10 to $\approx$110 points in 1/48th of the Brillouin zone) are studied, and it is found that the total energy usually converges to $\approx$1 millihartree when $\approx$30 **k** points are used. Cohesive energies are calculated (the hcp metals are taken to be fcc for this purpose). A cohesive energy is the difference in energy between the crystal and the free atom in its ground state; local density theory, as applied to the free atom, is usually appropriate to the *average* of a number of multiplet levels. For those cases where the promotion energy to this average can be estimated, the resulting cohesive energies are in accord with experiment. The fcc-bcc structural energy differences, taken as the difference in two total energies, are also calculated. These agree with experiment as to which structure is the more stable. There are no observed values for these differences but they are markedly greater in the middle of the 5*d* row than the generally accepted values, obtained in the course of constructing phase diagrams for alloys using regular solution theory. The present results suggest that these constructs should be reexamined. The *s*, *p*, and *d* orbital character of the occupied electron levels is also examined using a Mulliken population analysis, and the more standard analysis where the charge density, within a Wigner-Seitz sphere, is decomposed into *l* components. The Mulliken analysis indicates somewhat greater *d* occupancy. More notably it indicates much less *s* and more *p* character than the Wigner-Seitz cell analysis does for all the metals except for Au.

I. INTRODUCTION

The 5*d* elements Lu—Au form an interesting series for study. Their large atomic numbers make relativistic effects extremely important yet largely because of the lanthanide contraction their physical and chemical properties are often barely distinguishable from their 4*d* counterparts. For this reason they are experimentally difficult to isolate and two of them, Hf and Re, were only found in the 1920's by x-ray spectroscopy. Included in this set are the element with the largest cohesive energy, W, the ones with the largest densities (Os and Ir with densities about twice that of Pb), and the element which, by some criteria, is most resistant to corrosion, Ir.

With the exception of W, which has been a prototype for many years, there have been relatively few calculations of the electronic structure of these elements, presumably because of the importance of relativistic effects.

In this paper we present results of a systematic study of the cohesive energy and structural energy difference ($E_{\rm fcc}$-$E_{\rm bcc}$) of these elements using density-functional theory and the recently developed linear augmented-Slater-type-orbital method[1] (LASTO). This method has the virtue of retaining a physically appealing and interpretable labeling of the basis, while at the same time permitting systematic improvement in both the basis and potential. We include relativistic effects in the *j*-weighted average or scalar relativistic approximation, i.e., spin-orbit coupling is neglected in the conduction bands (though not the core) but all other relativistic effects (mass velocity, Darwin) are included to all orders. The recent pseudopotential calculation[2] of Bylander and Kleinman for W indicates that the cohesive energy increases by only 5 millihartrees out of 328 millihartrees when the spin-orbit interaction is included. (We use hartree atomic units, one hartree=27.212 eV.)

It is by now recognized that cohesive and structural energies are well described using the density-functional theory.[3] Examples include studies[4] of C, Si, and Ge by Yin and Cohen, calculation[5] of the zone-boundary phonons in Zr, Nb, and Mo by Ho *et al.*, and calculations on bulk W by Jansen and Freeman[6] and by Bylander and Kleinman.[2] Moruzzi, Janak, and Williams[7] have calculated the cohesive energies, atomic volume, and bulk moduli of the 3*d* and 4*d* row while Andersen and co-workers have given[8] the atomic volumes and bulk moduli for the 4*d* and 5*d* row.

Recently, Skriver[9] has calculated the structural energy differences for over 40 elemental metals using the LMTO method and Andersen's force theorem. He finds, as we do, that the crystal structures are correctly predicted in the 5*d* row with the exception of gold for which bcc is very slightly favored. Our calculations are based on the total-energy differences between the fcc and the bcc phases rather than the force theorem. Therefore, our results confirm the accuracy of the theorem for these metals. We have made a detailed comparison between force theorem and total-energy results elsewhere.[10] For example, it is well known[9] that the force theorem requires that the potentials in the atomic-sphere approximation (ASA)

be frozen and that there is a delicate cancellation between double-counted electrostatic terms in the two systems in this case (fcc and bcc). This leads to the result that the structural energy difference can be related to the sum of the one-electron eigenvalues (the band energy). However, we have shown that if the potentials are not frozen we obtain the same structural energy difference (within ~ 1 millihartree) but the eigenvalue sums do not reflect this difference.[10] In fact, judging by the self-consistent eigenvalue sums all of the $5d$ elements would be predicted to be fcc. This means that the force theorem may be a useful technique but that the interpretation of structural energy differences as "due to" differences in eigenvalue sums is questionable (although such an argument is given in Sec. III). We believe that there is not yet a wholly satisfactory physical explanation for the structural energy trends.

Our structural energy differences generally predict the observed crystal structure, but the magnitudes are significantly larger than often quoted values. For most of the elements the experimental structural energy differences are not known.

Cohesive energies are generally an order of magnitude larger than structural energy differences. On the other hand, uncertainties in precisely how to treat the atoms leads to relatively larger errors for the cohesive energy. Indeed, we find that the trend of the cohesive energy across the row is well reproduced by our calculations, but that the absolute value depends on how the atom is treated.

The details of the LASTO method have been presented in two previous papers[1,11] (denoted as I and II below). In Sec. II we review the method briefly and give results for various convergence tests we have performed, including choice of basis sets and convergence with respect to number of points in the Brillouin zone BZ. In general, we find ≈ 30 points uniformly spaced in the BZ to be adequate for ≈ 1 millihartree accuracy in the total energy. In Sec. III we discuss the structural energy difference and in Sec. IV the cohesive energies. Section V contains a summary of wave-function character and Sec. VI a conclusion

II. CALCULATIONS

A. Basis sets

The LASTO method employs a Bloch sum of Slater-type orbitals (STO's) of the form

$$\phi_{nlm}(\mathbf{r})=[(2\zeta)^{n+1/2}/\sqrt{(2n)!}]r^{n-1}\exp(-\zeta r)Y_{lm}(\mathbf{r}) \quad (1)$$

in the interstitial region of the crystal (between nonoverlapping spheres). Here the Y's are spherical harmonics and the prefactor is the normalization constant. The STO's are augmented within the spheres by numerical solutions of the "j-weighted average" Dirac equation. Therefore, there is a dual representation for the charge density. In the region outside the spheres it is given by a sum over the STO's which in turn depends on the number of functions included in the basis set. Inside the spheres it is given by a sum over angular momenta. We have found that including up to $\lambda_{\max}=8$ inside the spheres yields total energies converged to ≈ 1 millihartree.

For the region outside small basis sets are desirable in that only small matrices then need be constructed and diagonalized in the course of the band calculation, as well as providing a simpler physical interpretation of the results. However, there is a cost associated with such sets, namely they must be optimized if reasonable results are to be obtained. When doing a single calculation for some given element it may well be more economic to use a large basis set, such as in the linearized augmented-plane-wave (LAPW) method, than to do the number of calculations necessary to define an optimized small basis set. In this section we are concerned with obtaining such sets for use in future alloy calculations and to ascertain how well such sets do.

Minimum basis sets involve one s, three p, and five d STO's. It is plausible to assign them the principal quantum numbers, n, appropriate to the valence bands in question, but the ζ remain to be defined. In the case of a d band one might equate the log derivative of the STO to Andersen's criterion[8] for the center of gravity of the band, i.e.,

$$\mathscr{L}=\frac{1}{\phi}\frac{d\phi}{dr}=-\frac{(l+1)}{r_{\mathrm{WS}}}, \quad (2)$$

where r_{WS} is the radius of the Wigner-Seitz sphere. (In Andersen's calculations the atomic-sphere radius is taken to be r_{WS} and there is no interstitial crystal region, whereas here a muffin-tin potential with nonoverlapping spheres is used.) For s and p functions, Andersen recommends

$$\mathscr{L}=\frac{l}{r_{\mathrm{WS}}}, \quad (3)$$

so that the s-band log derivative has zero value corresponding to the bottom of the s band and the p-band $\mathscr{L}$ lies below the bottom of the p band (note that the occupied bands of a transition metal do lie below the onset of the unhybridized p band). Now the log derivative of an STO is

$$\mathscr{L}=\frac{n-1}{r}-\zeta, \quad (4)$$

so that we obtain

$$\zeta_s=\frac{n-l-1}{r_{\mathrm{WS}}}=\frac{n-1}{r_{\mathrm{WS}}}, \quad (5a)$$

$$\zeta_p=\frac{n-l-1}{r_{\mathrm{WS}}}=\frac{n-2}{r_{\mathrm{WS}}}, \quad (5b)$$

and

$$\zeta_d=\frac{n+1}{r_{\mathrm{WS}}} \quad (5c)$$

for s, p, and d functions, respectively. These are good first guesses for the ζ. The ζ's were then varied so as to minimize the total energy. It was found that Eq. (5a), evaluated[12] at r_s and not r_{WS}, suffices for ζ_s yielding total energies within a few tenths of a millihartree of the optimum choice. Similarly good energies were obtained when Eq. (5b) was replaced by

$$\zeta_p=\frac{n-1}{r_s}-\mathscr{L}+0.1. \quad (6)$$

This is only Eq. (4), evaluated[12] at r_s, and rewritten with an extra, empirically determined, factor of 0.1, where $\mathscr{L}$

is the p-shell log derivative calculated in the course of the band calculation. As might be expected, the total energies are more sensitive to the detailed choice of the ζ_d. The ζ_d values obtained and used in these calculations are plotted in Fig. 1. First consider the right-hand side of the figure. The ζ_d for Au with its filled d bands lie above Eq. (5c) although below its counterpart, evaluated at the muffin-tin rather than the WS sphere radius. In other words, the Andersen criterion, Eq. (2), appears to be working but for some radius intermediate between r_{WS} and the muffin-tin sphere radius, r_s. The bcc ζ_d lies higher than its fcc counterpart because the bcc r_s is smaller [hence $(n+l)/r_s$ is larger]. The ζ_d's drop with respect to Eq. (5c) upon moving left across the figure. Smaller ζ_d are, from Eq. (4), associated with $\mathscr{L}$ appropriate to energies *lowered* in the bands and thus ζ_d drops as the center of the *occupied* bands falls increasingly below the band center of gravity. This is what happens on moving left from Au to Lu.

Some idea of the sensitivity of the total energy to the choice of the ζ's is given in Fig. 2, where the total energy of fcc Ir is plotted as a function of ζ_p and of ζ_d. The ζ's based on Eqs. (5b) and (5c) are indicated and in this case they lead to total energies which are poorer, by 4 and 1 millihartree, respectively, than the energy of the optimum choice.

The effect of going to larger basis sets, with their concomitant increase in computing effort, has been investigated for a number of the $5d$ metals. Doubling the basis,[13] so that there are two s-, two p, and two d-like STO, was found to improve the total energy by 7 to 10 millihartrees. Adding an f-like STO, as well, produced a further improvement of 2 to 3 millihartrees. LAPW calculations effectively employ complete basis sets and comparisons, made in II for tungsten, indicated the LAPW total energy to be 2 millihartrees better than the seven STO result. While a total-energy improvement of the order of 10 millihartrees attends going from the optimized minimum set to the seven STO set, the calculated energy differences between the fcc and bcc structures, to be considered in Sec. IV, change by only 1 millihartree. It is anticipated that the minimum STO bases should provide accurate heats of alloy formation as well.

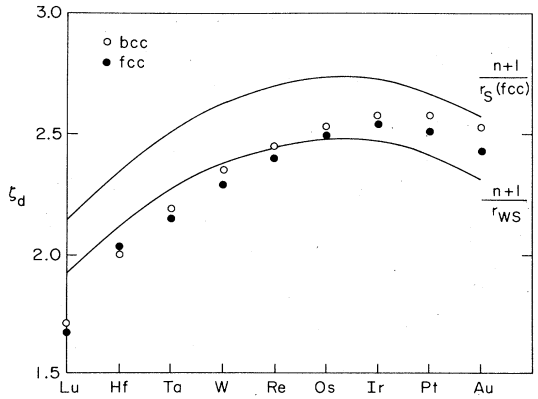

FIG. 1. Slater-type orbital ζ_d for the $5d$ transition metals in both the fcc and bcc structures. The two curves are Eq. (5c) evaluated with the Wigner-Seitz and with the fcc muffin-tin radii.

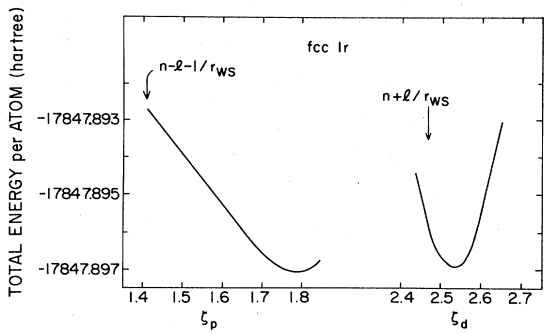

FIG. 2. Example of the sensitivity of the total crystal energy to the choice of the ζ when one s-like, one p-like, and one d-like STO is used. Shown is the dependence of the fcc Ir energy with varying ζ_p and ζ_d.

Linearized calculations also require the enrgy (or energies) at which the radial equation is integrated inside the muffin-tin spheres. The present calculations employed

$$\hat{\epsilon}=\frac{1}{N}\int_0^{\epsilon_F}\epsilon n(\epsilon)d\epsilon-0.04\,, \tag{7}$$

where $n(\epsilon)$ is the band density of states and N the number of valence electrons. In other words, $\hat{\epsilon}$ was taken to be the center of gravity of the occupied levels, with a shift downwards of 0.04 hartree. Such a shift was observed to produce a modest improvement in the total energy.

Lu presented particular problems because the one-electron energies of its $4f$ (core) levels lie inside the bands. These were treated as bands in the calculation (which caused no problem since they were completely occupied) and it became necessary to set $\hat{\epsilon}$ equal to the $4f$ level's energy. (Calculations where $\hat{\epsilon}$ was set equal to the $4f$ value when integrating the f-like radial equation while using a different $\hat{\epsilon}$ for the other l values produced an insignificant improvement in the total energy.)

B. k meshes

The calculations have been done for a number of meshes of special **k** points[14,15] ranging from the meshes of eight and ten points defined[14] by Chadi and Cohen for the bcc and fcc lattices to meshes of 112 and 110 **k** points for the two lattices, respectively. In all cases they are uniform cubic meshes which include **k** points on the (1,1,1) lines. The total energies, as a function of the separation of the **k** points (in x, y, or z), are plotted in Fig. 3 (the results for W have been reported in II and are not repeated here).

As a rule, calculations including $\approx$30 **k** points yield total energies which are within $\approx$1 millihartree of the calculations employing large numbers of **k** points. This is in contrast with the full-potential augmented-plane-wave (FLAPW) calculations[6] of Jansen and Freeman for W which employed the analytic linear tetrahedron method[16] (which samples by interpolation between calculated **k** points). They obtained total energies which increased by 2 and 5 millihartrees, when going from 30 to 90 mesh points, for bcc and fcc W, respectively, and they were able to extrapolate these to energies for infinitely fine meshes. Au is the only case for which there is a similar variation,

as indicated by the sketched in lines on Fig. 3, with varying special-point mesh size and the variation is markedly smaller in magnitude. It would appear that total energies for the fcc and bcc structures are better obtained with 30—40 special **k** points than with an equivalent number of points with the analytic linear tetrahedron method, although the latter provides a much more detailed depiction of the electron density of states. While the virtues of special **k** points are widely recognized, it is perhaps surprising that as few as 30 points do so well for the total energy of a transition metal with its partially occupied, rather flat, *d* bands.

III. STRUCTURAL ENERGIES

The bcc-fcc structural energy differences can be read off Fig. 3 and the resulting values are represented by the bottom edge of the hatched region of Fig. 4. These calculations were done with touching muffin-tin spheres and with a muffin-tin potential. Since there is a larger interstitial volume in the bcc structure, there arises the question of muffin-tin errors contributing to the structural energy differences. One measure of this is to employ the bcc spheres, which do not touch, in the calculations for the fcc structures. Taking the resulting total energies for the fcc leads to the values at the upper edge of the hatched region—having done a poorer job on the fcc total energies, the bcc structures are more favored.

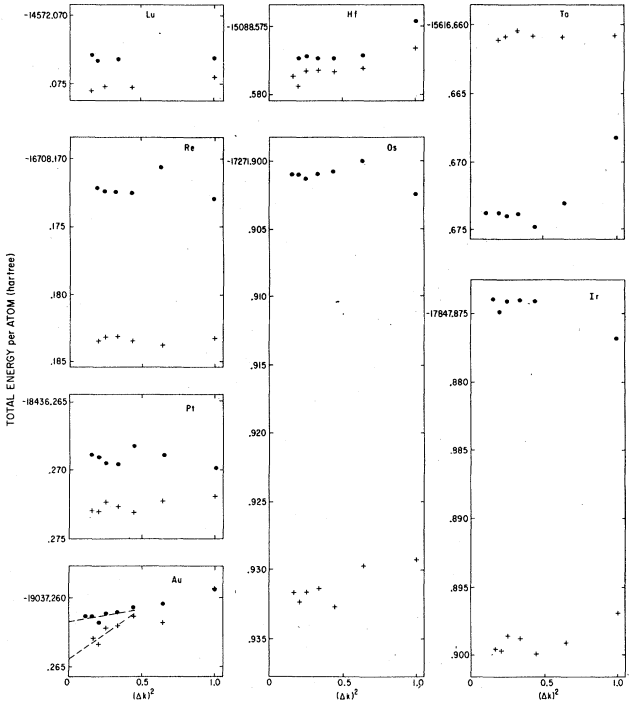

FIG. 3. Total crystal energies for the 5*d* metals (excluding W) as a function of the separation (squared) of the **k** points in the special **k** point meshes. The meshes associated with plotted points to the right of each plot correspond to the eight point fcc (the circles) and the ten point bcc (the crosses) meshes defined (Ref. 14) by Chadi and Cohen. The number of points at other separations can be read off the equivalent figure drawn for W in II. The lines in the Au plot are drawn to help the eye. For clarity, only the last three significant figures are shown on the *y* axes except for the topmost point.

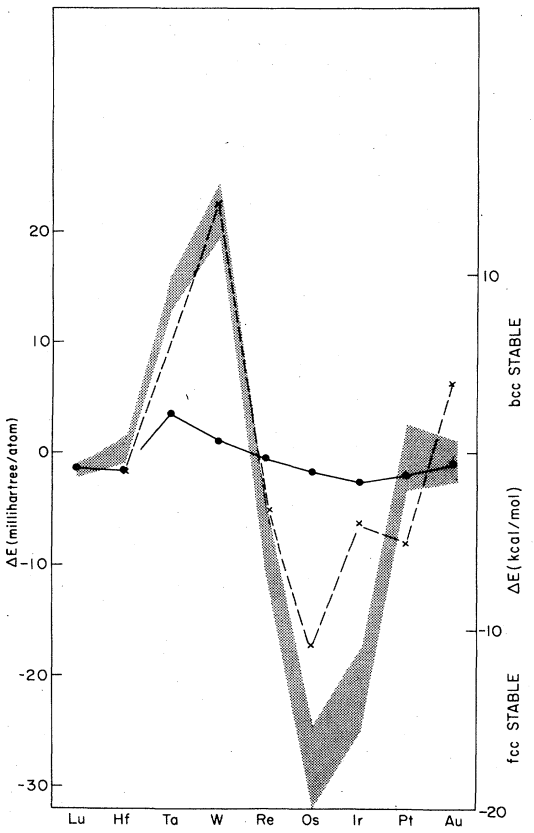

FIG. 4. fcc-bcc structural energy differences for the elements Lu though Au. The hatched region encompasses the present predictions as discussed in text. The solid line for Lu and Hf is the experimental hcp-bcc energy difference while the remainder of the line is based (Ref. 18) on fcc-bcc energy differences which bring regular solution theory into rough agreement with the experimental phase diagrams. The dashed line indicates hcp-bcc energy differences obtained in the Engel-Brewer model of transition-metal alloying (Ref. 19).

The energy differences defining the upper edge of the shaded region in Fig. 4 involved calculations for the fcc structures employing the bcc atomic spheres. As can be seen for the ζ_d's in Fig. 1, the basis set of ζ's change, somewhat, upon going from the bcc to the fcc structure. This raises the question of what ζ should be used with the bcc spheres in the fcc structure. Investigation had shown that it is the bcc ζ which are the optimal basis set in this case, this implying that the changing ζ are primarily associated with changes in r_s rather than with the changing structure. This would suggest that calculations, for other structures or for alloys, can be done with the combined set of an r_s and its associated ζ_i. Care must, of course, be taken if factors such as strong charge transfer arise. The

full-potential LAPW calculations[6] of Jansen and Freeman for fcc and bcc W give an energy difference of 21 millihartrees which is roughly midway between our two values. We presume that full-potential calculations for the other elements would also lie within the shaded area.

In all cases our calculation agrees with the observed crystal structure (if fcc is predicted then "observed" can be fcc or hcp). Possible ambiguities occur for Hf, Pt, and Au, where the structural energy differences approach the magnitude of our muffin-tin error. Unfortunately, there is almost no experimental data for the magnitude of the structural energy difference. Often quoted values[17,18] are given as the solid curve in Fig. 4, but with the exceptions of Lu and Hf where high-temperature hcp-bcc transitions are observed, they are not based directly on experiments. Rather they are obtained as fitting parameters in an analysis of the phase diagrams of alloys using regular solution theory[18] and, while in agreement for Pt and Au, they are markedly smaller than our values for Ta through Ir. An alternative approach[19] to the structural energy differences, based on the energies required to promote atoms to the various configurations deemed appropriate in the Engel-Brewer model to the structures in question, gives results (also given in Fig. 4) which are of the same scale as our calculations from Ta to Ir (but are larger for Pt and Au). The fact that the values based on regular solution theory seem low has been noted previously.[9,20,21] We believe that the present results, for the first time based on total-energy differences, necessitate the reexamination of the adequacy of regular solution theory as a model for the phase diagrams of transition-metal alloys.

The structural energy trend may be rationalized by comparison of the fcc and bcc electron densities of states. The $n(\epsilon)$ for bcc Ta and fcc Ir, decomposed into s, p, and d partial densities, appears in Fig. 5. The constructs involved band calculations employing a 112 point bcc and a 110 point fcc k mesh (in $\frac{1}{48}$ of the zones). Individual contributions were broadened by the derivative of the Fermi function with a temperature of 3 millihartrees or ≈ 1000 K as was used for W in II. (This function resembles a Gaussian with FWHM=0.3 eV). While there are peaks and hollows in the fcc $n(\epsilon)$, it is, in its gross features, a rectangle. In contrast, there is a large hollow in the bcc $n(\epsilon)$ with the Fermi level of Ta occurring at its onset and that of W close to its minimum. The occurrence of the Fermi level in a hollow implies that the occupied one-electron levels have been pushed to lower energy (and the unoccupied to higher) than is the case for an $n(\epsilon)$ of the same center of gravity and same overall width but without the hollow. This tends to maximize structural bonding energy. A similar hollow occurs in the $n(\epsilon)$ of the hcp structure (for which no calculations have been reported here). The Fermi levels of Re and Os fall in that hollow and they form in the hcp structure.

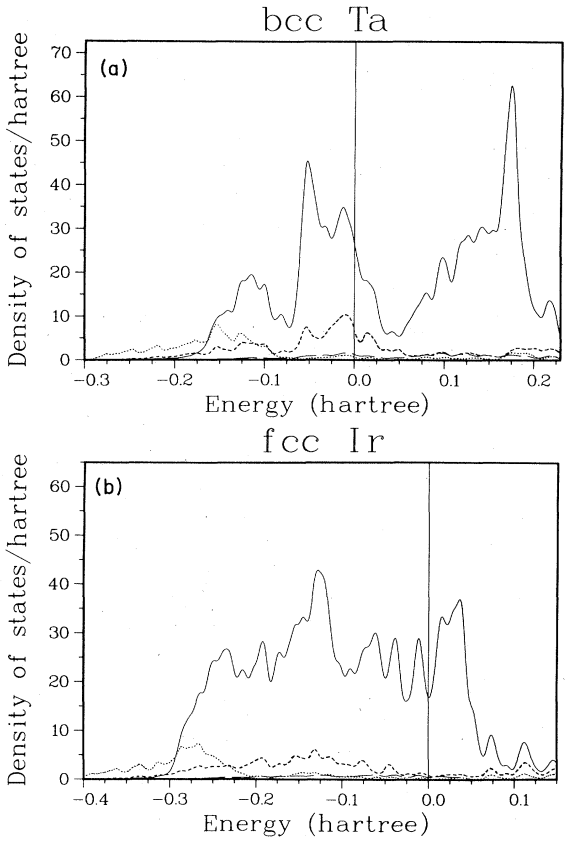

FIG. 5. s (dotted line), p (dashed line), and d (solid line) partial densities of states of bcc Ta and fcc Ir based on 112 and 110 **k** point meshes in $\frac{1}{48}$ of the respective Brillouin zones. The population weights were determined by a decomposition of an occupied orbital's spherical charge density within a Wigner-Seitz sphere into its $\lambda=0$, 1, 2, and 3 components. Individual histogram contributions were broadened by the derivative of the Fermi function corresponding to a temperature of 3 millihartrees or ≈ 1000 K.

IV. COHESIVE ENERGIES

The cohesive energy is the difference in energy between the ground state of the crystal and the free atom in its ground state. Such an energy difference is more difficult to calculate accurately than is the difference between two crystal energies such as the structural differences of the preceding section. One frequently cited reason for this is the *difference in errors* in applying local-density theory to a crystal with its moderate electron densities in the interstitial region versus applying it to a free atom with its low-electron-density tail. However, there are more serious problems than this, which are associated with the free-atom theory here. We are dealing with heavy elements for which relativistic effects are important: There exists no relativistic Hartree-Fock theory which properly describes a single Hund's rule multiplet level, and the problem is exacerbated on going to local-density theory. Such relativistic theories can deal with Shortley's average over an atomic configuration,[22] where the number of electrons in each shell with principal quantum numbers n and l (or n, l, and j) is assigned and where the m quantum numbers in each shell are averaged over. The problem, then, is that the calculated free-atom total energy is the center of gravity of a set of multiplet levels, and in calculating the cohesive energy one must estimate the promotion energy from the atom's ground state to that center of gravity. The scale of the problem is indicated in Fig. 6, where the

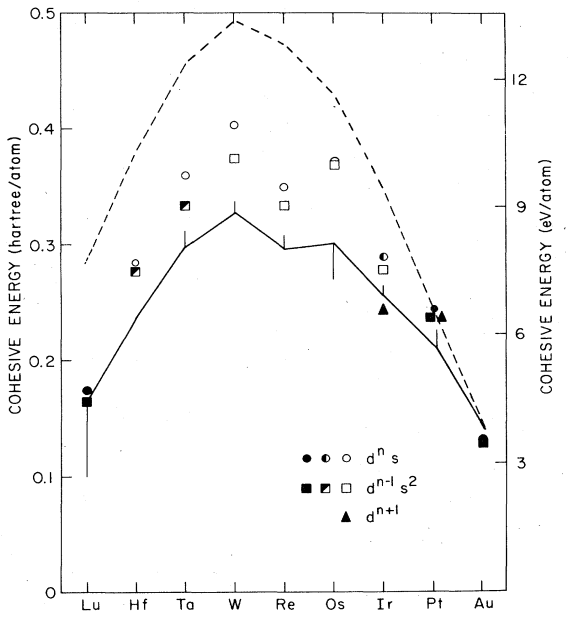

FIG. 6. Cohesive energies of the $5d$ metals (the hcp metals were treated as being fcc in these estimates). The solid curve is experiment as reported (Ref. 23) by Kittel while the vertical lines off it indicate other reported experimental values for these energies. The dashed curve is the calculated energy difference between the crystal and the free atom in the average of the $d^n s^1$ multiplet levels (as discussed in text). Lacking the promotion energy from the atom's ground-state multiplet to this average, this is *not* the cohesive energy. The plotted points involve various estimates of the promotion energy to the free-atom average of configurations as discussed in the text [the cohesive energy then being E(cryst)-E(av. of config.)-E(promotion)]. The promotion energies were estimated using spectroscopic data and the solid symbols indicate cases where the energies of all the multiplet levels of some configuration are listed, the half-filled where some are missing, and the open where the data is sparse (the high-lying multiplets tend to be missing, hence a cohesive energy is then overestimated).

solid line is the experimental cohesive energy as tabulated[23] by Kittel, and the dashed line the energy difference between the lowest-lying (fcc or bcc) crystal energy and the local-density free-atom $d^n s$ average of configuration total energy. That is, the atoms were not spin polarized and were fully (not scalar) relativistic. The configuration was d^{n+1}, $d^n s$, or $d^{n-1}s^2$. In order to compare with our scalar-relativistic solids the $d_{3/2}$ level had 0.4 of the d electrons. The difference between the two curves is primarily due to the free-atom promotion energy although there are contributions as well from any shortcomings in the calculations and in the experimental data. The crystal energies employed in Fig. 6 were obtained with the optimized three STO basis sets and going to the extended sets would have the effect of increasing the cohesive energies, i.e., raising the dashed line and points by 10—15 millihartrees atom. In addition, the nonmuffin terms would contribute[11] about 10 millihartrees (for W at least).

The promotion energies can, in principle, be obtained from either theory or experiment. Given the shortcomings of local-density theory and the availability of atomic spectra tables,[24] it would appear that the latter is the better choice. This is not altogether satisfactory because, more often than not, for the $5d$ elements, only some of the multiplet levels associated with a given configuration have been seen. There are also questions of whether all the multiplet assignments are correct and whether mixing between levels of like-symmetry shifts the energy of an individual level and hence of the configuration average obtained with it. The plotted points in Fig. 6 use the available multiplet data for the $d^n s$, $d^{n-1}s^2$, and d^{n+1} configurations to estimate promotion energies. These were then combined with the local-density energy. Solid symbols correspond to those cases where all the requisite multiplet levels are reported in the spectral tables, partially filled symbols when the data is almost complete, and the open symbols to where the multiplet data is sparse. Since it is the low-lying multiplets which tend to be reported for an incomplete set, using them then leads to an underestimate of a promotion energy. This causes the open symbols, associated with such cases, to lie highest above the experimental line as is seen. In the case of Pt a relativistic calculation in the $d^4_{3/2}d^5_{5/2}s$ configuration, spin restricted, moves the solid symbols down so that they lie on top of the experimental result.

As an alternative, we have followed Moruzzi, Janak, and Williams[7] (MJW) and calculated the cohesive energy using the spin-polarized atom energy. This was also the procedure followed by Jansen and Freeman for tungsten.[6] In the $5d$ row this is a sensible hybrid approximation where the core is treated fully relativistically but in the valence shell the spin-orbit interaction is turned off and spin polarization on. This approximates a single multiplet in tungsten (^7S) but not in Hf, Os, or Ir. There is, however, an added problem in the $5d$ row, namely the most of the $5d$ elements have $d^{n-1}s^2$ ground states while it is known that the local-spin-density (LSD) theory favors the $d^n s$ configuration.[25,26] In the $4d$ row most (although not all) of the elements have $d^n s$ configurations. Therefore, the LSD theory is expected to do worse on the $5d$ elements than the $4d$ elements. This is illustrated in Table I,

TABLE I. Cohesive energy of the $5d$ elements. $d^n s$ is the energy of the solid relative to the atom in the spin-restricted $d^n s$ configuration. LSD is the local-spin-density result obtained by subtracting the spin-polarization energy of the atom (Ref. 27). LSD$-E_{\rm pro}$ is further corrected by the experimental promotion energy to go from the ground state of the atom, $d^n s^2$ for Lu—Ir and $d^n s$ for Pt and Au, to the average of the $d^n s$ configurations with maximal spin. $E_{\rm Expt}$ is from Ref. 23. Energies in millihartrees equal 0.0272 eV.

Element	$E_{d^n s}$	$E_{\rm LSD}$	$E_{\rm LSD}-E_{\rm pro}$	$E_{\rm Expt}$
Lu	285	250	156	163
Hf	379	314	232	237
Ta	454	353	299	298
W	494	347	333	327
Re	473	375	310	295
Os	429	368	319	300
Ir	346	313	271	255
Pt	238	224	224	215
Au	135	130	130	140

where our solid energy relative to the scalar-relativistic spin-restricted $d^n s$ configuration is given in the first column. In the second column we have corrected for the spin polarization as tabulated by Brooks and Johansson.[27] The errors are generally larger than would be found for the $4d$ elements. In the third column we have corrected these results by the experimental promotion energy to go from the lowest multiplet level to the average of configuration for the $d^n s$ state with maximal spin.

For example in Ir, the excited states with $d^n s$ configuration and maximal spin make up two multiplets, ^4F and ^4P. Averaging over both of these yields a promotion energy of 42 millihartrees. Brooks and Johansson[27] also included promotion energies in their analysis but apparently used the lowest member of the multiplet, in this case $^4F_{9/2}$, which gives the promotion energy of 13 millihartrees.

This procedure reduces the errors considerably, and they are now of the same scale (actually somewhat smaller) as those reported by MJW.[7] This good agreement is partly the result of cancellation of errors between the local-density theory, which overestimates the cohesive energy and the muffin-tin approximation and basis-set errors in our calculations which underestimate it.[11]

V. WAVE-FUNCTION CHARACTER

We have analyzed the wave-function character of the occupied levels in two ways—a Mulliken population[28] and a Wigner-Seitz (WS) sphere population. The Mulliken population can be determined directly from the secular matrix which is

$$\sum_{N'} H_{NN'}C_{N'} = \epsilon \sum_{N'} S_{NN'}C_{N'} , \tag{8}$$

where H is the Hamiltonian, in our case (9×9) and S is the overlap matrix. N is a composite index giving the quantum numbers of the STO basis set. By definition the Mulliken population is

$$P_N = \sum_{N'} \mathrm{Re}(C_N^* S_{NN'} C_{N'}) . \tag{9}$$

Note that if S is diagonal then

$$P_N \propto |C_N|^2 , \tag{10}$$

which is the standard definition of a population using an orthonormal set.

The Wigner-Seitz (WS) population was determined from the charge density inside the muffin-tin spheres. Since the wave function is

$$\psi(\mathbf{r}) = \sum_N C_N \psi_N(\mathbf{r}) \tag{11}$$

and inside the spheres

$$\psi_N(\mathbf{r}) = \sum_{\lambda,\mu} \gamma_{N,\lambda\mu} f_\lambda(r) Y_{\lambda\mu}(\hat{r}) , \tag{12}$$

where the radial function $f_\lambda(r)$ is usually given in terms of another radial function g and its energy derivative $\dot{g}$ (see I and II). Consequently, the spherically averaged charge density inside the sphere has a natural decomposition in terms of $\lambda = 0,1,2,3$, etc. To obtain the WS population we have smoothly extended these densities out to the WS radius. We note that this is only a method of analyzing the charge density, the WS radius plays no other role in our calculations. In general, these WS populations do not add up to the valence charge, but for the close-packed systems we have studied, we find that they do to within a few tenths of an electron. The WS procedure has the virtue of being well defined. However, the tail of some orbital, of given l', centered off the site in question will appear to have quite different l character at the site being sampled, hence leading to some question of the physical meaning of such attributions. Also, when dealing with a compound, any attribution of the charge transfer between sites depends critically on the *choice* of site volumes. There are also problems with the Mulliken population analysis[28] because it must deal with the nonorthogonality of orbitals centered on different sites and employ some scheme to apportion wave-function character granted that nonorthogonality. Such an analysis, of course, depends on the orbitals, hence the STO ζ's, which were chosen so as to optimize the crystal energy. While the absolute values of l population counts resulting from such analyses should not be taken too seriously, the *changes* in population with changing compound or crystal structure should be meaningful, particularly if the calculations employ common basis sets. One virtue of applying such analyses to compounds is that they define the charge associated with orbitals *centered* on some site, and this is the natural way to define the ionic character of the compound.

As expected, the d electron count is incremented by ≈ 1 from element to element on traversing the $5d$ row. (Only small changes are obtained in the occupation numbers on going from the fcc to the bcc structures for a given element.) The Wigner-Seitz cell analysis for fcc Lu yields a d count of $1.45e$ which is incremented by values slightly less than 1 on going up to fcc Os which has a value of $6.22e$. Then the increments are slightly greater than 1 with fcc Au having a d count of $9.39e$. The Mulliken analysis yields values which range from $0.3e$ greater for Lu to $0.05e$ greater for Ir, Pt, and Au.

The WS cell analysis yields non-d electron counts which lie between $1.55e$ and $1.75e$ across the row. Small amounts of this charge are associated with higher l but the bulk is s and p like. The s counts are almost constant, between $0.82e$ and $0.89e$ and the p counts range between $0.67e$ and $0.92e$, thus indicating roughly equal s and p character in the bands. The situation is quite different with the Mulliken population analysis, as can be seen for W in Fig. 7. The s count is much less, namely ≈ 0.3 for Lu through Os, then rising to 0.7 by Au. The p counts are roughly 4 times the s for the first half of the row and drop to a factor of 2 larger for Pt while being almost equal for Au. Bylander and Kleinman employed[2] the Löwdin orbital-population analysis[29] to their calculation for W and obtained a disparity in s-versus-p occupation similar to that here.

It has been recognized for some time that the d count in the transition metals is markedly less than the count appropriate to the $d^n s^1$ atomic configuration. Important

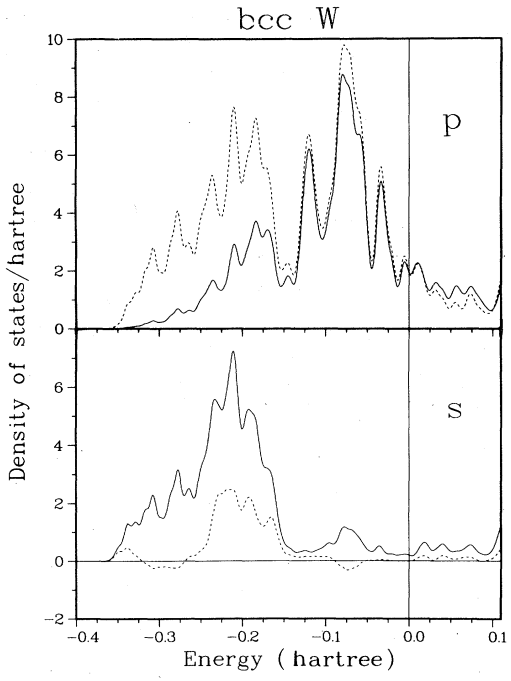

FIG. 7. s and p partial densities of states for bcc W employing the Mulliken population analysis (dashed histograms) and the Wigner-Seitz population analysis (solid histograms). Individual histogram contributions have been broadened as in Fig. 5 and the results are based on a sampling of 112 special **k** points in 1/48th of the Brillouin zone. The s Mulliken population goes negative (though slightly) in several places. As is well known, this is due to the way the Mulliken scheme handles the nonorthogonality between orbitals centered on different sites.

to this is the hybridization of non-d character with the d bands, particularly for the lower-lying portion of the d bands. This allows, for example, a metal such as Au with its filled d band to have less than ten d states per atom throughout the eleven states per atom in the occupied bands. Lacking orbital-population analyses, the balance of s and p orbital behavior has been less obvious until now. The large-p (versus s) occupations obtained by Bylander and Kleinman[2] for W and obtained here would suggest that the hybridization in the lower d bands is largely d-p in character. Inspection of Fig. 7 supports this: There is little s character, except in the vicinity of -0.2 hartree below the Fermi level and little s or p above. The lack of s or p character at energies overlying the upper half of the d bands is important to the relatively constant s and p population counts across the $5d$ row. It is difficult to define the exact lower bound of the d bands but it is in the vicinity of -0.25 hartree. Granted this, it would appear that the depletion of s character, as obtained in the Mulliken versus the WS sphere analysis, is associated with the lowest-lying levels both above and below the onset of the d band. While viewing Fig. 7 it must be remembered that, though the orbital-population analysis may make more chemical sense than a sampling within a WS sphere, the results do depend on the scheme employed to handle orbital nonorthogonality. Nevertheless, there is the strong suggestion that the d-band hybridization is primarily d-p in character. The modification of this when an atom has unlike nearest neighbors should be an important aspect of compound formation.

At this point we note that there is a long-standing disparity between the band-theory description of transition metals and the Pauling-Engel-Brewer view[19] which associates fcc metals such as Pt and Au with $d^{n-2}(sp)^3$ configurations, hcp with $d^{n-1}(sp)^2$ configurations, and bcc with $d^n s$. It might be argued that the disparity is due to the almost universal use of WS-type populations rather than Mulliken type in the band- theory literature. However, our Mulliken populations tend to side with the band-theory description on this issue. For example, we find a remarkable constancy in the non-d electron count across the row which is inconsistent, within the Pauling-Engel-Brewer picture, with the observed crystal-structure trend. Also as discussed in Sec. III the structural energy differences are readily understood in terms of differences in the d-band density of states. Finally, the d count while roughly the same in the WS and Mulliken senses is nevertheless slightly *larger* for the Mulliken, which is less in accord with Pauling-Engel-Brewer theory than the more traditional estimates of band populations.

CONCLUSION

To summarize, we have utilized a new method in band theory to calculate the cohesive and structural energies of the $5d$ transition elements. Our scalar-relativistic muffin-tin potential results complement the cohesive energies calculated previously for the $3d$ and $4d$ rows.[7] However, since $d^{n-1}s^2$ configurations predominate in the $5d$ row over $d^n s$ (which local-density theory favors), we find it important to include the appropriate promotion energies. Having done so, our results agree slightly better with experiment than those of Moruzzi, Janak, and Williams.[7] This good agreement is partly due to cancellation of errors between the local-density theory (which overestimates cohesion) and the muffin-tin and basis-set errors in our calculations.

Our structural energy differences, which are based on total energies, confirm Skriver's[9] LMTO—force-theorem results. Both show that muffin-tin potentials do correctly predict the proper crystal structure of these elements with the exception of gold. However, the magnitude of the structural energy is larger by an order of magnitude than the often quoted "experimental" values of Kaufmann. This disagreement is not a muffin-tin effect (by comparison with the full-potential results for tungsten). Therefore, we believe that the "experimental" values should be reexamined. In most cases they are not actually measured but are derived from fitting the results of regular solution theory to the phase diagrams of alloys.

ACKNOWLEDGMENT

This work was supported by the Division of Materials Sciences, U.S. Department of Energy under Contract No. DE-AC02-76CH00016.

[1]J. W. Davenport, Phys. Rev. B **29**, 2896 (1984).
[2]D. M. Bylander and L. Kleinman, Phys. Rev. B **27**, 3152 (1983); **29**, 1534 (1984).
[3]*Theory of the Inhomogeneous Electron Gas,* edited by S. Lundqvist and N. H. March (Plenum, New York, 1983).
[4]M. T. Yin and M. L. Cohen, Phys. Rev. Lett. **45**, 1004 (1980); Phys. Rev. B **26**, 5668 (1982).
[5]K.-M. Ho, C. L. Fu, B. N. Harmon, W. Weber, and D. R. Hamann, Phys. Rev. Lett. **49**, 673 (1982).
[6]H. J. F. Jansen and A. J. Freeman, Phys. Rev. B **30**, 561 (1984).
[7]V. L. Moruzzi, J. F. Janak, and A. R. Williams, *Calculated Electronic Properties of Metals* (Pergamon, New York, 1978).
[8]A. R. Macintosh and O. K. Andersen, in *Electrons at the Fermi Surface,* edited by M. Springford (Cambridge University Press, Cambridge, 1980).
[9]H. L. Skriver, Phys. Rev. B **31**, 1909 (1985).
[10]M. Weinert, R. E. Watson, and J. W. Davenport Phys. Rev. B **32**, 2115 (1985).
[11]J. W. Davenport, M. Weinert, and R. E. Watson, preceding paper, Phys. Rev. B **32**, 4876 (1985).
[12]This implies that the ζ changes on going from one atomic sphere to another of different radius. A constant ζ would be expected if a single STO were an exact representation of the wave function, which as we know from atomic experience it is not. The change in the ζ here is in the direction expected, namely ζ is larger at smaller radii, i.e., the STO is less screened when closer to the nucleus.
[13]The ζ of the extra STO are reasonably well chosen by Eq. (5c) for $6d$-, $7s$-, $7p$- and $5f$-like STO's. Optimization of these ζ, and modification of the first set of three ζ, has of the order of a 1 millihartree effect on the total energy.
[14]D. J. Chadi and M. L. Cohen, Phys. Rev. B **8**, 5747 (1973).
[15]H. J. Monkhorst and J. D. Pack, Phys. Rev. B **13**, 5188 (1976).
[16]O. Jepson and O. K. Andersen, Solid State Commun. **9**, 1763 (1971); G. Lehman and M. Taut, Phys. Status Solidi **54**, 469 (1972).
[17]R. Hultgren, P. D. Desai, D. T. Hawkins, M. Gleiser, and K. K. Kelley, *Selected Values of the Thermodynamic Properties of Binary Alloys* (American Society for Metals, Metals Park, Ohio, 1973).
[18]L. Kaufman and H. Bernstein, *Computer Calculation of Phase Diagrams* (Academic, New York, 1970).
[19]L. Brewer, in *Phase Stability in Metals and Alloys,* edited by P. S. Rudman, J. Stronger, and R. I. Jaffee (McGraw-Hill, New York, 1967). Brewer attributes integral electron counts to the various crystal structures here and these are what we cite in text. Nonintegral values are often employed for the boundaries between structures in the Engel-Brewer construct.
[20]D. G. Pettifor, J. Phys. C **3**, 367 (1970).
[21]See the discussion on pages 148—150 of Ref. 18.
[22]G. H. Shortley, Phys. Rev. **50**, 1072 (1936).
[23]C. Kittel, *Introduction to Solid State Physics,* 5th ed. (Wiley, New York, 1976).
[24]C. E. Moore, *Atomic Energy Levels,* Natl. Bur. Stand. (U.S.) Spec. Publ. No. 35. (U.S. GPO, Washington, D.C., 1971).
[25]J. Harris and R. D. Jones, J. Chem. Phys. **68**, 3316 (1978).
[26]D. M. Bylander and L. Kleinman, Phys. Rev. Lett. **51**, 889 (1983).
[27]M. S. Brooks and B. Johansson, J. Phys. F **13**, L197 (1983).
[28]R. S. Mulliken, J. Chem. Phys. **23**, 1833 (1955).
[29]P. O. Löwdin, J. Chem. Phys. **18**, 365 (1950).